# Experimental Study of a Pressure-Driven, Three-Dimensional, Turbulent Boundary Layer

Shawn D. Anderson* and John K. Eaton†
*Stanford University, Stanford, California*

**This paper presents the results of an experimental investigation into a strongly skewed, pressure-driven, three-dimensional turbulent boundary layer. The investigation is undertaken in order to further the physical understanding of such three-dimensional flows and to provide a detailed data set as a support to computational modeling efforts. Mean velocity and static pressure measurements reveal the general nature of the flowfield studied, while detailed measurements of the Reynolds stress tensor with an X-array hot wire indicate the effect of the strong pressure gradients on the turbulent velocity field. Two separate regions of the flow are investigated in depth: the plane of symmetry along the centerline of the facility and a freestream streamline passing through a region of highly skewed flow. The results from the streamline investigation show that the magnitude of the Reynolds shear stresses relative to the normal stresses drops off under the influence of the three-dimensionality, and the shear vector lags strongly behind the velocity gradient vector. Both of these effects are felt to be dominated by the rate at which the boundary layer is skewed and reflect changes in the essential nature of the flow which cannot be captured by simple modifications of two-dimensional flow models.**

## Nomenclature

$A1$ = $\sqrt{\overline{u'v'}^2 + \overline{v'w'}^2}\,/q^2$
$B_x$ = dimensionless pressure gradient parameter = $\delta_{99}(\partial C_p/\partial X)$
$C_f$ = skin friction coefficient = $2\tau_w/(\rho U_e^2)$
$C_p$ = static pressure coefficient
$H$ = boundary-layer shape factor
$N$ = ratio of eddy viscosities = $\nu_c/\nu_s$
$q^2$ = twice turbulent kinetic energy = $\overline{u'^2} + \overline{v'^2} + \overline{w'^2}$
$R$ = local radius of curvature of freestream streamline
$U$ = $X$ component of mean velocity
$U_e$ = local $U$ velocity at the edge of the boundary layer
$U^+$ = nondimensional shear layer velocity = $U/\sqrt{\tau w/\rho}$
$V$ = $Y$ component of mean velocity
$W$ = $Z$ component of mean velocity
$\overline{u'^2}$ = $xx$ component of Reynolds stress
$\overline{v'^2}$ = $yy$ component of Reynolds stress
$\overline{w'^2}$ = $zz$ component of Reynolds stress
$\overline{u'v'}$ = $xy$ component of Reynolds stress
$\overline{u'w'}$ = $xz$ component of Reynolds stress
$\overline{v'w'}$ = $yz$ component of Reynolds stress
$x$ = coordinate direction along freestream streamline
$X$ = coordinate direction along tunnel centerline
$y$ = coordinate direction normal to wall
$Y$ = coordinate direction normal to wall
$Y^+$ = nondimensional shear layer wall normal = $(Y\sqrt{\tau w/\rho})/\nu$
$z$ = coordinate direction perpendicular to freestream streamline
$Z$ = coordinate direction perpendicular to tunnel centerline
$\delta_{99}$ = boundary-layer thickness
$\nu_c$ = cross-stream eddy viscosity; $\nu_c = -(\overline{v'w'})/(\partial W/\partial Y)$; m$^2$/s
$\nu_s$ = streamwise eddy viscosity; $\nu_s = -(\overline{u'v'})/(\partial U/\partial Y)$; m$^2$/s
$\tau_w$ = wall shear stress

Presented as Paper 86-0211 at the AIAA 24th Aerospace Sciences Meeting, Reno, NV, Jan. 6–9, 1986; received May 21, 1986; revision received Dec. 10, 1986. 

*Research Assistant, Mechanical Engineering. Member AIAA.
†Associate Professor, Mechanical Engineering. Member AIAA.

## Introduction

PRESSURE-DRIVEN, three-dimensional, turbulent boundary layers are a common feature in the flow over the external surfaces of modern aircraft. Advances in the fields of computational fluid dynamics and computer design have allowed designers to make increasingly accurate predictions of complex flows, but many obstacles to the successful computation of three-dimensional viscous flows remain. The behavior of the turbulent Reynolds stress tensor is particularly difficult to model in three-dimensional flows. This work focuses on the behavior of a turbulent boundary layer as it reacts to a known pressure field, with the general objective of providing a useful data set to guide efforts aimed at improving the models used to represent the turbulence structure of complex flows.

The behavior of pressure-driven three-dimensional flows has been a topic of research for over 30 years. Johnston[1] reviewed the available experiments and found few data sets which included detailed Reynolds stress data. Johnston and van den Berg[2] both made the observation that the shear-stress vector was usually found to lag the velocity gradient vector in a pressure-driven three-dimensional boundary layer. Viewed from the standpoint of a simple flow model, this means that the eddy viscosity in the spanwise direction is less than that in the streamwise direction. The ratio of the eddy viscosities has been found to vary from flow to flow and too few data sets are available to determine what controls the lag of the stress vector, or even to quantify the nature of the lag itself.

In a discussion of research into the flow over an "infinite" swept wing, Bradshaw and Pontikos[3] raised another issue: the fact that the magnitude of the shear stress is seen to decrease as the flow moves through the three-dimensional region. They suggest that this observation may be explained by examining the effect the three-dimensionality of the flow has on the large eddy structures of an originally two-dimensional shear layer. At present there is insufficient experimental evidence to support a complete understanding of the actual behavior of these types of flows.

There is a clear need for further data sets which address the questions just raised, but there are major problems in obtaining such data sets. Measurement of the full Reynolds stress tensor in a three-dimensional boundary layer, particularly the cross-stream shear-stress component $\overline{v'w'}$, is very difficult. Careful studies (e.g., Driver and Hebbar[4]) show that three-component laser-Doppler anemometer (LDA) systems can systematically underestimate the shear-stress correlation coefficients by 10–20%. Hot-wire anemometer measurements which are usually made with X-array probes are subject to spatial resolution problems. In addition, hot-wire signal analysis techniques require the assumption that turbulence levels are small relative to the mean flow and usually neglect the effect of velocities parallel to the wire. Nevertheless, carefully applied hot-wire techniques employing digital data reduction and frequent recalibration can supply full stress tensor measurements with a reasonable level of uncertainty. A second major problem is the interpretation of the large amount of data needed to define a three-dimensional flow. Modern computational techniques are now supplying a framework to interpret such data.

The overall objectives of the present research program are to provide physical insight into the behavior of three-dimensional boundary layers and to produce new data for the qualification of three-dimensional computational procedures. A test case was sought in which an initially two-dimensional boundary layer was skewed by a spanwise pressure gradient and was also subject to an adverse streamwise pressure gradient. The specific test case chosen for this work is one in which an initially two-dimensional boundary layer is distorted by the pressure field of a wedge facing into the flow (see Fig. 1). This configuration yields a strong spanwise pressure gradient and an adverse streamwise pressure gradient leading to separation on the centerline near the wedge tip. The configuration chosen also has the advantage of having a plane of symmetry which can be used as a boundary in computations, provides a good check of the measurement procedures, and is an interesting test case in itself.

The specific objectives of the program are as follows:

1) To map the mean flow behavior of the wedge flow including static pressure data and two components of the mean velocity field.

2) To measure the evolution of the Reynolds stresses in the planes perpendicular to the surface and parallel to two streamlines; one being the centerline and the other being a freestream streamline indicated in Fig. 1.

3) To provide all boundary-condition documentation needed to compute the flowfield using statistical computational techniques.

Complete documentation of the experiment is available in Ref. 5.

## Experimental Apparatus

### Three-Dimensional Turbulent Boundary Layer Facility

The experimental facility consists of a development section to generate a two-dimensional turbulent boundary layer and a test section where the three-dimensional character of the flow is developed and explored. A sketch of a side view of the wind-tunnel layout is shown in Fig. 1. A low-turbulence airflow enters the boundary-layer development section from a 4.8 : 1 contraction and passes through the development section, which is a 2.1 m long, 12.7 × 61 cm rectangular duct. The boundary layer flow then encounters the pressure field generated by the 90 deg included-angle wedge facing into the flow and by flexible fairings extending downstream from the development section end-walls (see Fig. 1). The fairings serve two purposes in this experiment. Their primary purpose is to eliminate the separation that would otherwise occur at the sudden expansion of the flow into the test section. They also provide another degree of control over the streamwise pressure gradient in the test section. For ease of description in

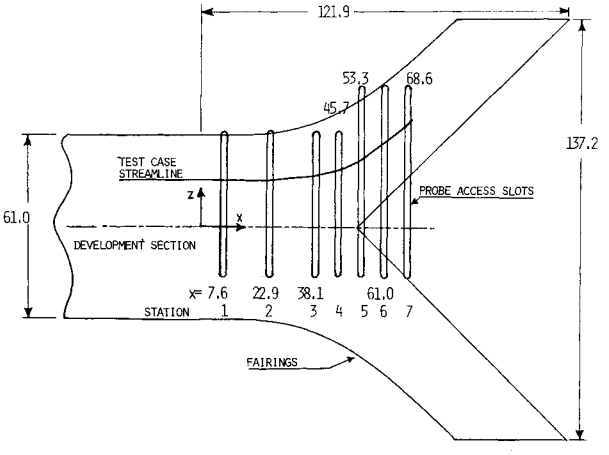


Fig. 1 Side-view sketch of a test section. Dimensions in cm.

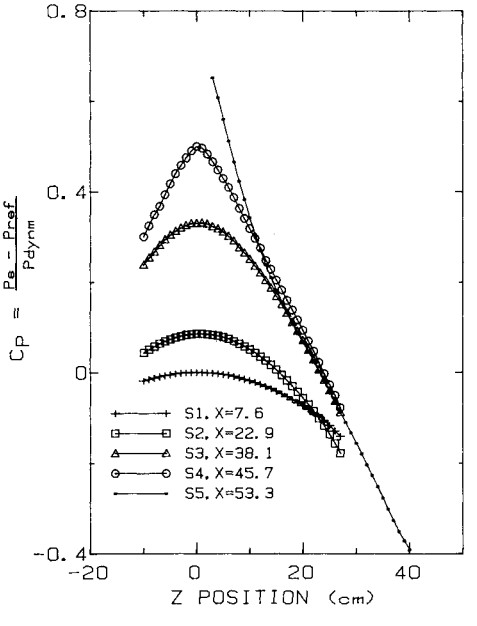


Fig. 2 Static pressure distribution at first five $X$ stations.

computational models, the position of the fairing position is insured by the use of a template to set the two fairings to the same shape. The symmetry achieved in this flow is excellent (see Results and Discussion section).

All tunnel surfaces are constructed of plexiglass which results in an apparatus having excellent optical access in all regions of interest. The current configuration allows instrument access through seven spanwise slots in the wall opposite the test wall. These slots are indicated in Fig. 1. A computer-controlled traverse mechanism provides spanwise and normal probe motions in addition to manual probe rotations in the $X$-$Z$ plane.

### Instrumentation

Three instruments are used to obtain the data set for this experiment: a standard static-pressure probe to map the pressure field, a three-hold yaw probe to obtain the mean velocity field throughout the region of interest, and a rotatable X-array hot-wire probe for measurement of the full Reynolds stress tensor. The static pressure probe is a United Sensor Corp. Model PSA-12 with 0.16-cm-diam stem. The probe is mounted in a goose-neck holder to allow determination of the static pressure field directly under the probe access slots.

The yaw probe is a standard three-hold pressure probe built using 0.8-mm diam hypodermic tubing. This probe is also

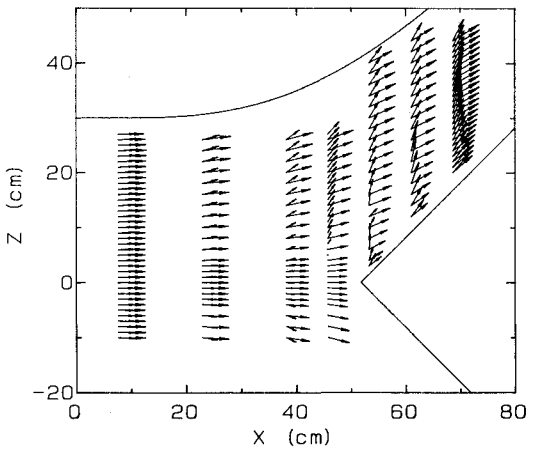


**Fig. 3 Mean velocity vector plots: freestream (long arrows, $Y = 5.93$ cm) and wall planes (short arrows, $Y = 0.19$ cm).**

constructed in a goose-neck configuration. A direct calibration of both velocity magnitude and yaw angle has been implemented which allows the probe to measure the velocity vector accurately provided the flow direction is within $\pm 30$ deg of the probe orientation. The actual practice followed in making the mean measurements was conservative; the probe was always orientated to within $\pm 25$ deg of the mean velocity direction. The presence of large velocity gradients near the solid surface causes errors in the yaw-probe measurements. By using a correction developed by Young and Maas[6] and implemented by Eibeck and Eaton[7], an effective location for the probe tip was calculated based on the measured gradient near the wall. The total uncertainty in the yaw-probe measurements is estimated to be $\pm 0.2$ m/s in the velocity magnitude and $\pm 1.0$ deg in the velocity vector angle. This translates into an uncertainty of $\pm 0.2$ m/s in the $X$ component and $\pm 0.3$ m/s in the $Z$ component of velocity.

A special X-array hot-wire probe which allows rotation about the stem axis is used for measurement of the full Reynolds stress tensor. The probe was built using a DISA 55P51 dual-sensor hot-wire tip having 3 mm long, 5 $\mu$m diam wires. The wires are gold-plated to achieve an active length of 1.25 mm, giving a length/diameter ratio of 250. The hot wire was mounted in a goose-neck stem which allows it to be yawed without translating the tip of the probe. Having both the yaw probe and the hot wire built in the same configuration allows measurements to be made with both probes in exactly the same location.

The hot-wire calibration and data acquisition are carried out under the control of the MINC PDP11-03 laboratory computer and follows the same procedure as was used by Westphal and Mehta[8]. In this procedure, the effective wire angles for each wire are determined in each of the four planes of measurement. Calibrations of the wire angles and velocity response relations were made before and after each profile and the run rejected if the calibration changes by more than 1%. The effect of ambient temperature drift on the hot-wire response is accounted for in the reduction process by a simple temperature correction to the measured voltage following the development of Bearman[9].

The probe is yawed at each measurement point so that the axis of the probe is always oriented to within two degrees of the mean velocity vector direction as determined from the yaw-probe measurements. All the components of the mean velocity vector and the Reynolds stress tensor are measured by rotating the plane of the wires into four separate positions: the $U$-$V$ plane, the $U$-$W$ plane, and two 45 deg planes. With the probe in the $U$-$V$ plane, the mean velocity components $U$ and $V$ and the Reynolds stress terms $\overline{u'^2}$,$\overline{v'^2}$, and $\overline{u'v'}$ are determined. The measurement of $W$ and $\overline{w'^2}$ and $\overline{u'w'}$ Reynolds stresses, along with redundant realizations of $U$ and $\overline{u'^2}$, are obtained in the $U$-$W$ plane. Measurements made in the two 45 deg planes are used only to obtain the remaining cross-flow shear stress, $\overline{v'w'}$. Implicit in this approach is the assumption that the sensitivity of the probe to the component of velocity along the sensor is negligible.

Quantification of the uncertainties present in X-wire measurements represents a more difficult task than making the measurements themselves. An extensive treatment of the origin and magnitude of the different uncertainties as well as a complete description of the calibration and acquisition procedure used are found in Anderson[5]. If we summarize that analysis, the effects accounted for include uncertainties due to probe misalignment, temperature drift, probe calibration uncertainties, and statistical variations. The results of the analysis for a series of typical turbulent velocity profiles indicate that mean velocities have an uncertainty of 2% of the local $U$, except near the wall in the skewed region, where the uncertainty approaches 3%. The Reynolds normal stresses have a calculated uncertainty which is always less than 4% of the local value of $\overline{u'^2}$. The Reynolds shear stresses have calculated uncertainties of less than 8%, except near the wall in the skewed boundary layer, where the uncertainties approach 12% of the local value of $\overline{u'v'}$.

As a check on the effect of the out-of-plane velocity components, two profile measurements were made in the inlet section; in the first the X wire was aligned with the flow direction, in the second run the X wire was deliberately misaligned by 5 deg. The reduction program was used to calculate the turbulent and mean velocity fields from both runs. Mean velocity results differed by less than 1.0% of the local $U$ velocity. The Reynolds normal stresses, $\overline{u'^2}$, $\overline{v'^2}$, and $\overline{w'^2}$ were within 4% of the $\overline{u'^2}$ stress, and the $\overline{u'v'}$ and $\overline{u'w'}$ shear stresses were within 7.5% of the local $\overline{u'v'}$ value. The largest discrepancy noted was in the value of $\overline{v'w'}$ near the wall, which showed a difference of 8.5% of the local $\overline{u'v'}$ magnitude. Comparisons of the X-wire mean velocity measurements with the three-hold probe measurements were made for over 1000 measurement locations, with no deviation larger than 2% being noted.

Based on the considerations just presented, the following uncertainties are assigned to the measurements made with the X wire. Mean velocities have an uncertainty level of no more than 3% of the local streamwise velocity. Reynolds normal stresses are judged to have an uncertainty of 5% and the Reynolds shear stresses have uncertainties of 10%, except $\overline{v'w'}$ which is felt to be subject to higher uncertainties especially near the wall, and assigned a value of 15% of $\overline{u'v'}$.

## Results and Discussion

### Boundary Conditions and Inlet Boundary Layer

Full documentation of the boundary conditions is available in Anderson[5]. These data include the exact geometric specification of the test facility, boundary-layer profiles on all four walls of the inlet duct, and three-component mean velocity measurements across the exit plane. All the data referred to next were measured with a freestream velocity in the inlet section of 16 m/s.

The boundary layer at the inlet is two-dimensional except those areas near the top and bottom surfaces which were affected by the fairing boundary layers. The inlet boundary layer has a thickness of approximately 3 cm, a momentum-thickness Reynolds number of 3700, and a shape factor of $H = 1.36$. The inlet boundary layer profile closely matches the conventional log law:

$$U^+ = 2.44 \ln Y^+ + 5.0$$

The friction velocity, $U_\tau$, was determined by fitting the measured velocity profile to the log law within the $Y^+$ range of $50 \le Y^+ \le 150$.

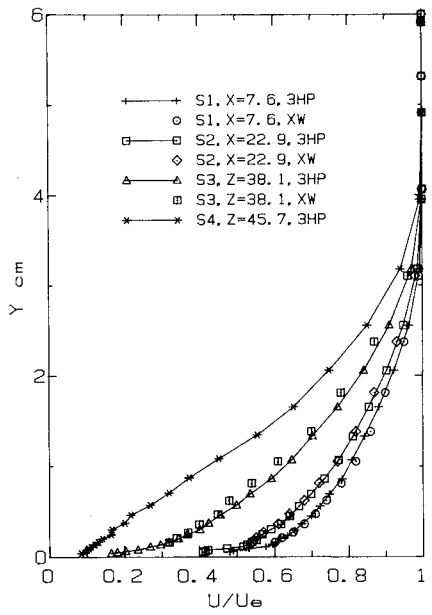


**Fig. 4 Streamwise mean velocity profiles on centerline: three-hole probe measurements (3HP) and X-array hot-wire measurements (XW).**

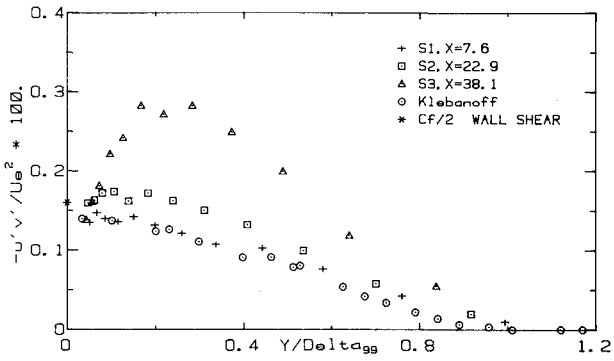


**Fig. 5 Streamwise Reynolds stress profiles on centerline; comparison with wall shear stress, $C_f/2$, and data of Klebanoff[10].**

The turbulence data were compared to the data of Klebanoff[10], which were taken in a boundary layer with a momentum-thickness Reynolds number of approximately 1400. The comparisons are presented next with the remainder of the turbulence measurements. The shear-stress measurements were found to be virtually identical to Klebanoff's data, whereas the kinetic energy data were up to 15% higher in the present experiment.

### Mean Flowfield

The three-dimensional boundary-layer development is driven by the pressure field imposed by the wedge and the fairings. The freestream ($Y > 1.5\delta_{99}$) static pressure distribution referenced to the centerline pressure at slot one and normalized by the freestream total pressure is shown in Fig. 2. The wall static pressure was measured at various locations and compared to the freestream measurements. These comparisons revealed that there is essentially no static pressure variation normal to the wall except in the region immediately upstream of the wedge. The static pressure data show that there is a very strong adverse pressure gradient along the channel centerline. For example, the dimensionless pressure gradient parameter $B_x$ has a value on the order of 0.02 between the second and third slots. The strong pressure gradient leads to separation in the vicinity of the fourth slot. The magnitude of the spanwise pressure gradient is in the same range as the streamwise gradient, meaning that the skewing of the boundary layer should be quite pronounced and rapid. The pressure gradient along the fairing is nearly zero as planned. The overall symmetry of the flowfield is also indicated by the results in Fig. 2, with the measured $C_p$ on either side of the centerline always matching to within 2%. The measured flow angles along the centerline nowhere exceed 0.5 deg, another indication of the flow symmetry.

Extensive measurements of the mean velocity field were made using the three-hole yaw probe. Spanwise surveys were made at five different Y locations for each of the seven X stations. Two of these five planes of data, the freestream plane at $Y = 5.93$ cm and the plane nearest to the wall at $Y = 0.19$ cm, are presented in Fig. 3. The longer vectors in this figure correspond to the freestream velocities. The two-dimensional character of the inlet boundary layer and the extent of the fairing boundary layer are readily apparent in the measurements from the first X station. The three-dimensional character of the test boundary layer develops between slots 1 and 5 where progressively stronger skewing of the near-wall flow is observed. By station 5, the relative flow angle between the freestream and the wall flow exceeds 40 deg. This region of rapid skewing between the first and fifth stations is the primary area of interest for the Reynolds stress measurements as next reported.

The flow can no longer be characterized as a boundary layer in the region just upstream of the wedge or across the entire span of the flow at stations 6 and 7. In these regions, there is a significant normal velocity component and axial gradients can be quite large. The normal velocity component is caused by separation upstream of the wedge tip, while it is caused by overall circulation in the downstream angled duct. A study of the flow in a plane at the exit of the test section was made using a four-hole probe capable of measuring all three components of the mean velocity. The measurements revealed a pair of large-scale circulation cells filling the flow passage. In addition to the spanwise mean velocity surveys, approximately 40 two-component mean velocity profiles were measured at various points in the test section. Selected profiles will be shown for the centerline flow and for the selected streamline.

### Centerline Flow

An interesting subcase for this work is the behavior of the flow along the centerline of the tunnel. This boundary layer experiences a strong deceleration with the magnitude of the freestream velocity decreasing monotonically by 20%. The development of the mean flow is indicated by the mean velocity profiles shown in Fig. 4. Throughout this paper, the local freestream velocity, $U_e$, is chosen as the quantity used to normalize both velocity and stress measurands. These profiles show features typical of a two-dimensional adverse pressure gradient boundary layer including a rapid thickening of the boundary layer and a retarded flow near the wall. Incipient separation is evident in the fourth X-station profile. X-array hot-wire measurements of the mean velocity were made at the first three X stations along the centerline and were found to agree with the yaw-probe results.

The streamwise Reynolds shear stress $\overline{u'v'}$ also develops much like that in a two-dimensional separating boundary layer (see Fig. 5). As the boundary layer develops, the peak rapidly grows larger and moves away from the wall. The shear-stress value near the wall falls as the skin friction decreases approaching separation. These data are very similar to data presented by Simpson et al.[11] for a two-dimensional separating boundary layer. The turbulent kinetic energy (Fig. 6) shows generally the same behavior as the $\overline{u'v'}$ shear stress. The other two shear-stress components $\overline{v'w'}$ and $\overline{u'w'}$ are expected to be zero on the centerline. The normalized values of $\overline{v'w'}$ are all less than 0.01, indicating that the measurement uncertainty is relatively low. The measured values of $\overline{v'w'}$ are slightly higher but still less than 0.03 for all but two measurements.

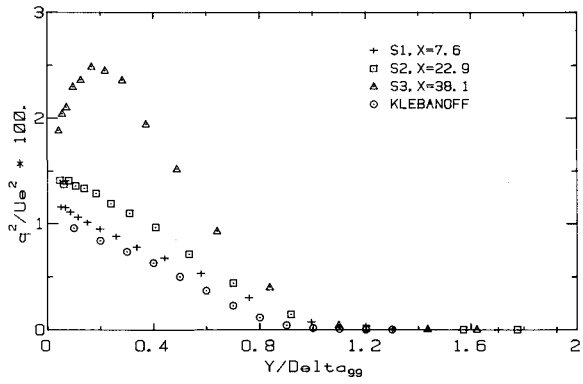


**Fig. 6 Turbulent kinetic energy profiles on centerline, comparison with data of Klebanoff[10].**

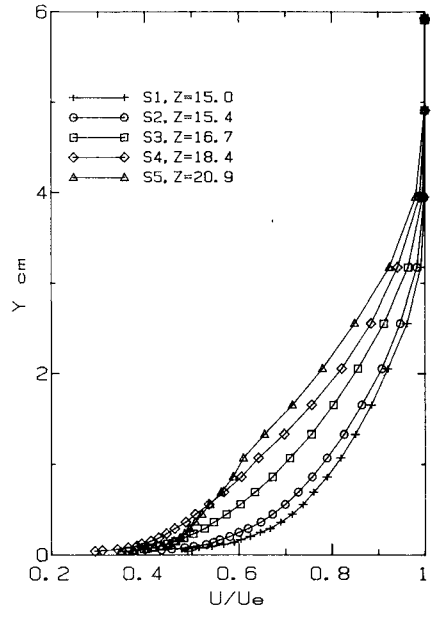


**Fig. 7 Streamwise mean velocity profiles on 15 cm streamline. Freestream streamline coordinates.**

The surface shear stress was determined by fitting the mean velocity profile to the log law and was also measured by the use of a surface fence gage described by Higuchi[12]. The value of the wall shear stress, presented as $C_f/2$, is also plotted in Fig. 5. The profile of $\overline{u'v'}$ may be extrapolated to the measured value of the wall shear stress.

### Flow Along the Selected Streamline

In addition to the study of the flow on the centerline, the flow along a freestream streamline originating 15 cm above the centerline was also investigated. This streamline was selected because it passes through the region of strong skewing but remains outside the separation zone near the tip of the wedge. The spanwise gradients in the vicinity of the streamline are also relatively small. In all subsequent plots, the data are presented in an $x, y, z$ coordinate system where $x$ is aligned with the local streamwise velocity, $y$ is normal to the wall, and $z$ completes a right-handed system. The mean velocity profiles measured at the first five $x$ stations are plotted in $U/U_e$ vs $y$ and $W/U_e$ vs $y$ coordinates in Figs. 7 and 8. These figures show the same flattening of the streamwise velocity component profiles as was observed along the centerline, owing to the adverse pressure gradient in the streamwise direction. The flow along the streamline experiences a strong deceleration through the first four slots, the freestream velocity decreasing by 10%, but begins to accelerate again as the

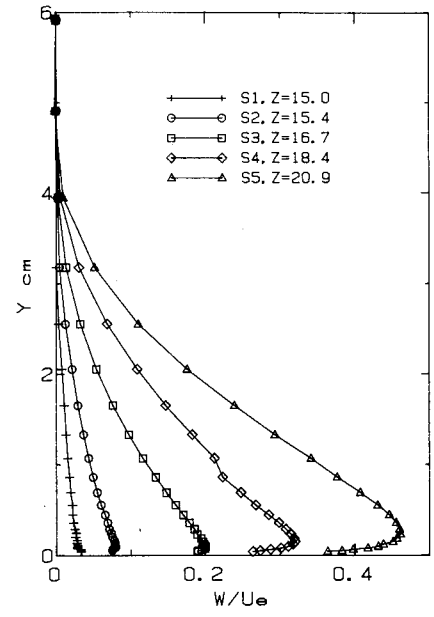


**Fig. 8 Cross-stream mean velocity profiles on 15 cm streamline. Freestream streamline coordinates.**

flow enters the exit passage alongside the wedge as is evident in the shape of the $U/U_e$ profile at the fifth slot. In addition to the adverse streamwise pressure gradient, there is a strong lateral pressure gradient driving the cross-stream velocity.

The behavior of the Reynolds stresses in this complex flow domain is a most interesting feature of this study. The behavior of the turbulent kinetic energy profiles is indicated in Fig. 9. A measure of the anisotropy of the normal stresses is given in Fig. 10, which presents profiles of the quantities $\overline{u'^2}/q^2$ and $\overline{w'^2}/q^2$ at the first, fourth, and fifth $x$ stations. The magnitude of $\overline{v'^2}/q^2$ may be inferred as the three should sum to one. Of the three normal stresses, the spanwise component, $\overline{w'^2}$, increases by the largest proportion. The $\overline{u'^2}$ stress increases with downstream development, but becomes a smaller fraction of the overall kinetic energy. The maximum turbulent kinetic energy on the streamline occurs at the fifth slot and exceeds the maximum value on the centerline by approximately 20%.

The development of the streamwise and cross-stream shear stresses in this same region may be seen in Figs. 11 and 12. The differences between the centerline and the streamline flow cases are most clearly seen in the behavior of these shear stresses. The dominant shear-stress component, $\overline{u'v'}$, no longer increases uniformly in the downstream direction. The peak in the $\overline{u'v'}$ stress level occurs at the fourth $x$ station and decreases slightly by the last measurement station. The shape of the profiles is also altered, the peak moving away from the wall and the levels near to the wall decreasing more than was observed in the centerline case. The cross-stream shear stress, $\overline{v'w'}$, exhibits an interesting development along this streamline. The level of $\overline{v'w'}$ remains essentially zero for the first two $x$ stations and then begins to have a negative value near the wall at the third station. When the flow has reached the fifth measurement station, there is a significant amount of positive $\overline{v'w'}$ stress in the center of the boundary layer. The sign of the stress may be understood by considering the sign of the gradient of the cross-stream velocity component in that region. Attention should be paid to the scaling of the plots of these stresses; in order to highlight the development of the individual stresses, the figures have different scales.

### Discussion

The results from the centerline study suggest that the three-dimensionality of the plane-of-symmetry flow does not have a

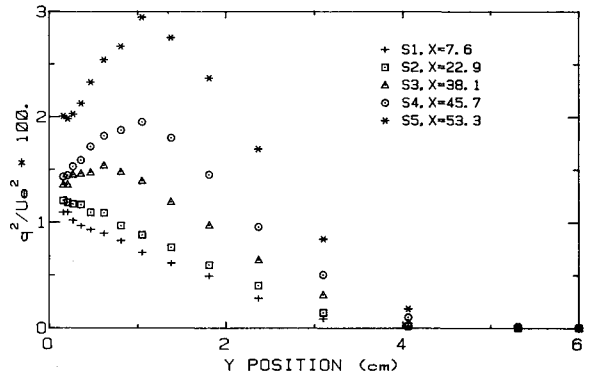


Fig. 9 Turbulent kinetic energy profiles on 15 cm streamline. Freestream streamline coordinates.

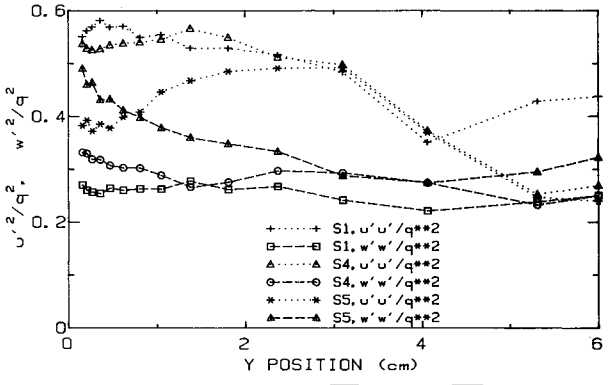


Fig. 10 Reynolds normal stresses, $\overline{u'^2}/q^2$ and $\overline{w'^2}/q^2$, on 15 cm streamline. Freestream streamline coordinates.

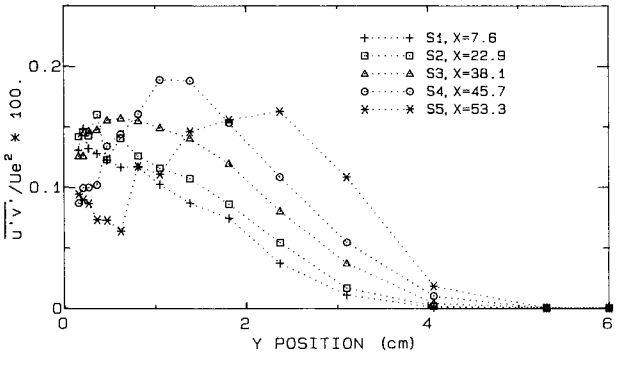


Fig. 11 Streamwise Reynolds shear stress $\overline{u'v'}$ on 15 cm streamline. Freestream streamline coordinates.

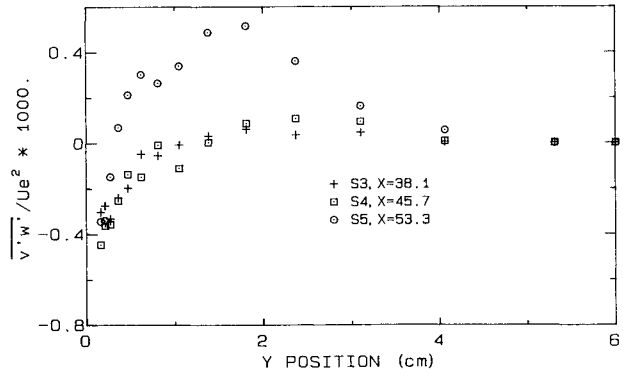


Fig. 12 Cross-stream Reynolds shear stress $\overline{v'w'}$ on 15 cm streamline. Freestream streamline coordinates.

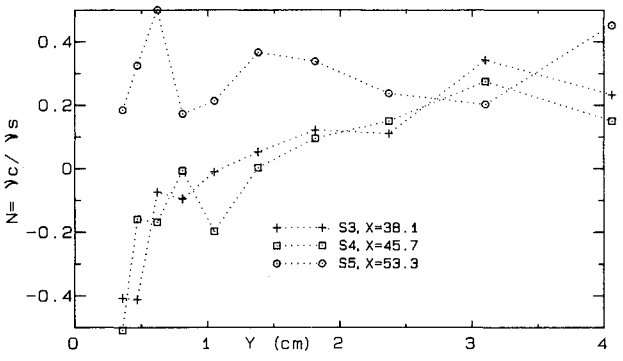


Fig. 13 Ratio of cross-stream eddy viscosity to streamwise eddy viscosity, $N = \nu_c/\nu_s$ on 15 cm streamline. Freestream streamline coordinates.

strong effect on the development of the turbulence. The development is quite similar to that of an ordinary two-dimensional separating boundary layer. Apparently, the effects of three-dimensionality are dominated by the strong effects of the adverse pressure gradient. Unfortunately, data are not available in the vicinity of the separation zone at the tip of the wedge. Turbulence structure modifications caused by the imposition of three-dimensionality may have a very significant effect on the extent and character of separation zones.

The data on the curved streamline exhibit more interesting behavior. When the data are examined in the coordinate system aligned with the local freestream velocity as just presented, the cross-stream shear stress, $\overline{v'w'}$, remains quite small except in a thin layer immediately adjacent to the wall. Away from the wall, $\overline{v'w'}$ is essentially zero until the last measurement station is reached. Even at station 5, the peak level of $\overline{v'w'}$ is only about one-fourth of the peak level of $\overline{u'v'}$. This level of the cross-stream shear stress is comparable to levels found in previous studies; e.g., Bradshaw and Pontikos[3]. The gradient of the spanwise velocity in the present case, however, is much larger than in that work.

A useful comparison to data from previous experiments can be made on the basis of the streamwise and cross-stream eddy viscosities. The streamwise eddy viscosity is defined as $\nu_s = -(\overline{u'v'})/(\partial U/\partial Y)$ and the cross-stream eddy viscosity is $\nu_c = -(\overline{v'w'})/(\partial W/\partial Y)$. The streamwise eddy viscosity changes slowly; there is some increase in the magnitude of the eddy viscosity in the outer region of the boundary layer, but the overall shape of the profile remains the same. The cross-stream component of the eddy viscosity is somewhat surprising in its development. The overall level of $\nu_c$ is very low, a factor of four below the peak levels of $\nu_s$. There is in fact no appreciable magnitude of $\nu_c$ until the last measurement station. These results are presented in Fig. 13 as the ratio of the cross-stream to the streamwise eddy viscosities, $N = \nu_c/\nu_s$. Others have found values of this ratio which range from approximately 0.1 to 1.0 (see Ref. 1.). The value of $N$ at the fifth $x$ station was approximately 0.2 in this study. This result is significant in that it highlights directly the problems of using isotropic eddy viscosity models in complex flows with only the current level of understanding of their behavior.

Another useful parameter to consider in understanding the results presented is the structural parameter, $A1$, defined as the ratio of the shear stress to the turbulent kinetic energy. We have based $A1$ on the vector magnitude of the two important shear stress components, $\overline{u'v'}$ and $\overline{v'w'}$. A plot of this parameter for the five measurement stations along the streamline is given in Fig. 14. The value of $A1$ at the first $x$ station is 0.15, the expected value for a two-dimensional turbulent boundary layer. As the flow develops downstream, however, the magnitude of $A1$ drops off dramatically. A drop in the magnitude of the Reynolds shear stresses relative to the normal stresses was also noted by Bradshaw and Pontikos[3], but a much larger decrease was found in the present case. The actual magnitude

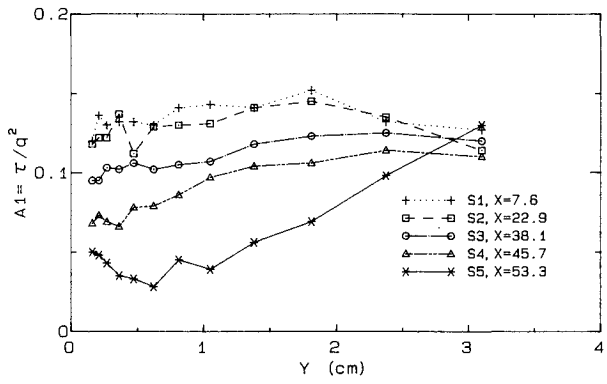


**Fig. 14 Structural parameter $A1 = \tau/q^2$ on 15 cm streamline.** $\tau = \sqrt{\overline{u'v'}^2 + \overline{v'w'}^2}$, $q^2 = \overline{u'^2} + \overline{v'^2} + \overline{w'^2}$.

of the shear stresses increases downstream, but not nearly as fast as the increase along the centerline. Also, the normal stresses increase much more rapidly than the shear stress, leading to the decrease in $A1$.

The data presented here indicate that the turbulence structure is out of equilibrium with the velocity gradient. Both the angle and magnitude of the velocity gradient vector change rapidly as the flow moves along the streamline. The shear stresses, especially the cross-stream shear stress $\overline{v'w'}$, are apparently not effectively extracting energy from the mean velocity gradients. The result is indicative of the disturbing effect the introduction of three-dimensionality has on the original structure of the two-dimensional boundary layer. On the other hand, the normal stresses respond rapidly to the changing velocity gradient. In particular, the spanwise normal stress $\overline{w'^2}$ increases very rapidly in response to the imposition of a gradient in the spanwise velocity component. This increase in $\overline{w'^2}$ is responsible for the rapid increase in the level of the turbulent kinetic energy. A simple argument suggests that $\overline{w'^2}$ would respond almost immediately to an increase in $\partial W/\partial Y$; spanwise motions caused by any turbulence structure would result in large values of $\overline{w'^2}$. However, the same argument fails to explain the behavior of the shear stresses for this flow.

The development of the third shear-stress component, $\overline{u'w'}$, is generally considered to be uninteresting because it does not appear in a boundary-layer formulation of the problem. In the present case, the $\overline{u'w'}$ component becomes as much as three times larger than $\overline{u'v'}$. Even at these high levels of $\overline{u'w'}$, however, the streamwise and spanwise gradients of the $\overline{u'w'}$ stress are still small relative to the normal gradients of the $\overline{u'v'}$ and $\overline{v'w'}$ stresses.

A key question which emerges from consideration of these results is: What parameters of a three-dimensional flowfield affect the development of the Reynolds stresses? One important parameter affecting the behavior of the stresses appears to be a non-dimensional rate of freestream turning, $\delta_{99}/R$, where $R$ is the local radius of curvature of the freestream streamline. Values for this parameter range from 0.001 to 0.005 for the present experiment, increasing with downstream development. Pontikos,[13] with a relatively low level of turning, $\delta_{99}/R = 0.01$, found values of the eddy viscosity ratio $N$ which sometimes exceeded 1.0, but had a typical value of $N = 0.75$. Johnston[14] found viscosity ratios of the order of 0.1 to 0.2 in a flow with higher rates of turning, $\delta_{99}/R = 0.04$. A possible reason, then, for the low value of $N$ in the present experiment is the very rapid turning rate that the flow experiences. The drop in $A1$ observed in this flow is also larger than that found in other experiments with lower turning. Another parameter which may be significant for understanding the behavior of the skewed boundary-layer flows is the magnitude of the skew angle, or the differential turning of the flow between the freestream and the wall. The effect of these two parameters on the development of the turbulent boundary layer will be examined in the near future by studying a less rapidly turned flow produced in the same facility with a narrower wedge.

## Summary

Results of an experimental investigation into the behavior of a pressure-driven three-dimensional turbulent boundary layer have been presented. Careful experimental procedures have been used to obtain data sets for two subcases. The results on the centerline indicate that the turbulence responds mainly to the adverse pressure gradient approaching separation at the wedge tip. There is no obvious influence of the three-dimensional turbulence field on the plane of symmetry flow. Data from the streamline passing through the region of high skewing demonstrate two main effects: The magnitude of the Reynolds shear stresses relative to the normal stresses drops off under the influence of the three-dimensionality, and the shear vector lags strongly behind the velocity gradient vector. Both of these effects are felt to be dominated by the rate at which the boundary layer is skewed and reflect changes in the essential nature of the flow which cannot be captured by simple modifications of two-dimensional flow models.

## Acknowledgments

We gratefully acknowledge the financial support of the NASA Ames Research Center under Contract NCC 2-238. We have had many useful discussions with our project monitor, Dr. Dennis Johnson. The first author has been supported partially through a three-year graduate fellowship from the National Science Foundation. Finally, we thank our colleague Professor James Johnston for numerous contributions to this work.

## References

[1]Johnston, J.P., "Experimental Studies in Three-Dimensional Boundary Layers," Thermosciences Div., Stanford Univ., Stanford, CA, Rept. MD-34, July 1976.

[2]van den Berg, B., "Some Notes on Three-Dimensional Turbulent Boundary Layer Data and Turbulence Modelling," *Three-Dimensional Turbulent Boundary Layers, Proceedings of the International Union of Theoretical and Applied Mechanics Symposium*, edited by H.H. Fernholz and E. Krause, Springer-Verlag, Berlin, 1982, pp. 1–18.

[3]Bradshaw, P. and Pontikos, N.S., "Measurements in the Turbulent Boundary Layer on an 'Infinite' Swept Wing," *Journal of Fluid Mechanics*, Vol. 159, Oct. 1985, pp. 105–130.

[4]Driver, D.M. and Hebbar, S.K., "Experimental Study of a Three-Dimensional, Shear-Driven, Turbulent Boundary Layer Using a Three-Dimensional Laser Doppler Velocimeter," AIAA Paper 85-1610, July 1985.

[5]Anderson, S.D., "An Experimental Investigation of Pressure-Driven, Three-Dimensional Turbulent Boundary Layers," Ph.D. Thesis, Stanford Univ., Stanford, CA, June 1987.

[6]Young, A.D. and Maas, J.N., "The Behavior of a Pitot Tube in a Transverse Total Pressure Gradient," Aeronautical Research Council, London, Rept. 1770, 1936.

[7]Eibeck, P.A. and Eaton, J.K., "An Experimental Investigation of the Heat-Transfer Effects of a Longitudinal Vortex Embedded in a Turbulent Boundary Layer," Thermosciences Div., Stanford Univ., Stanford, CA, Rept. MD-48, Nov. 1985.

[8]Westphal, R.V. and Mehta, R.D., "Crossed Hot-Wire Data Acquisition and Reduction System," NASA TM 85871, Jan. 1984.

[9]Bearman, P.W., "Corrections for the Effect of Ambient Temperature Drift on Hot-Wire Measurements in Incompressible Flow," DISA Electronics, Franklin Lakes, NJ, Rept. 11, May 1971, pp. 25–30.

[10]Klebanoff, P.S., "Characteristics of Turbulence in a Boundary Layer with Zero Pressure Gradient," NACA TN 3178, July 1954.

[11]Simpson, R.L., Strickland, J.H., and Barr, P.W., "Features of a Separating Turbulent Boundary Layer in the Vicinity of Separation," *Journal of Fluid Mechanics*, Vol. 79, March 1977, pp. 553–594.

[12]Higuchi, H., "A Miniature, Directional Surface-Fence Gage for Three-Dimensional Turbulent Boundary Layer Measurements," AIAA Paper 83-1722, July 1983.

[13]Pontikos, N.S., "The Structure of Three-Dimensional Turbulent Boundary Layers," Ph.D. Thesis, Imperial College, London, 1982.

[14]Johnston, J.P., "Measurements in a Three-Dimensional Turbulent Boundary Layer Induced by a Swept, Forward-Facing Step," *Journal of Fluid Mechanics*, Vol. 42, July 1970, pp. 823–844.